

Computational Fluid Dynamics Lab 2

ME 207 | Fluid Dynamics

Diya Mehta 22110078, Nishit Mistry 22110172, Shrishti Mishra 22110246, Utkarsh Srivastava 221100278, Vatsal Trivedi 22110276

1. Problem Statement

Consider laminar flow over a NACA 0012 airfoil section. The chord length of the airfoil is 1 meter. The freestream velocity is 30 m/s, and the air temperature is 25°C. The density and dynamic viscosity of air are approximately 1.225 kg/m³ and 1.81×10^{-5} Pa·s, respectively.

2. Geometry and Boundary Conditions

2.1. Geometry Conditions

The geometry of the simulation domain consists of a NACA 0012 airfoil section with the following dimensions:

- Chord length: 1 m

The NACA 0012 airfoil serves as a representative airfoil section for analyzing the aerodynamic performance of a wing or an aircraft in laminar flow conditions.

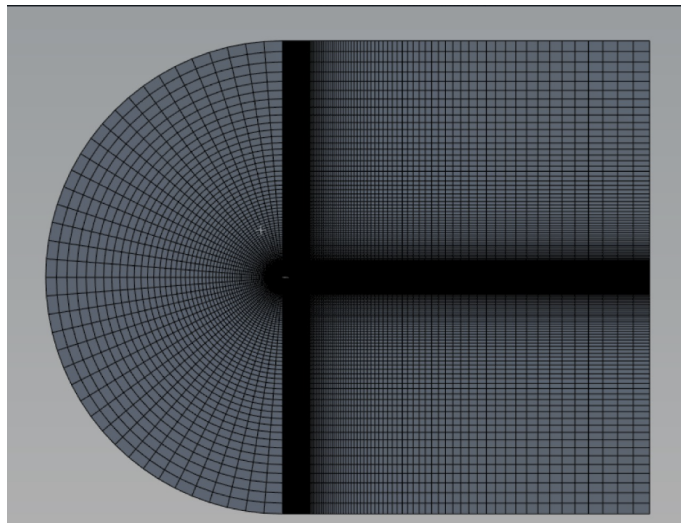


Figure 1. 2.1 Mesh Geometry

2.2. Boundary Conditions

The boundary conditions applied to the simulation are crucial in defining the flow characteristics within the pipe. They are as follows:

- Inlet Boundary Condition: At the inlet of the computational domain, specify the freestream velocity and temperature. Since the flow is assumed to be fully developed and uniform at the inlet, use a velocity inlet boundary condition with the given freestream velocity of 30 m/s and the air temperature of 25°C.
- Outlet Boundary Condition: At the outlet of the computational domain, apply a pressure outlet boundary condition. This boundary condition allows the flow to exit the computational domain freely, assuming that the pressure at the outlet is ambient or atmospheric pressure.
- Wall Boundary: For the surfaces of the airfoil (upper and lower surfaces), apply a no-slip wall boundary condition. This condition assumes that the velocity of the fluid at the

surface of the airfoil is equal to the velocity of the airfoil itself, resulting in zero velocity relative to the airfoil.

3. Mesh Statistics and Mesh Independence Study

A mesh independence study is conducted to ensure that the results are not significantly affected by the mesh resolution. Several levels of mesh refinement are employed, with increasing mesh density. Mesh statistics including the number of nodes and elements are recorded for each refinement level.

drag_coefficient_2	
Cd	
airfoil	
Cd	0.0087245827
lift_coefficient_2	
C1	
airfoil	
C1	8.6302259e-05

Figure 2. 3.1 Cd and Cl for nodes = 17280

Statistics	
Nodes	17280
Elements	17040

Figure 3. 3.2 Nodes and Elements

In this case, to analyse mesh independence, we'll analyse the value of Cd (Drag Coefficient) and Cf (Lift Coefficient),

Nodes	Elements	Cd	Cf
17280	17040	0.0087	8.63e-05
34340	34000	0.0069	2.49e-05
68160	67680	0.0057	1.93e-06

Table 1. Mesh Independence Study

As can be observed, the value of Cd and Cf does change, although not drastically, for different mesh sizes. This concludes that though not initially but mesh independence, is gradually achieved.

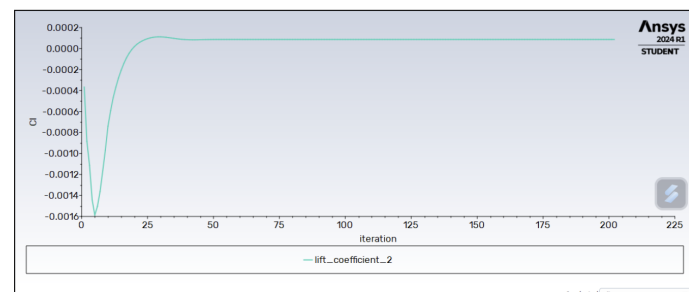


Figure 4. 3.3 Cd plot for nodes = 17280

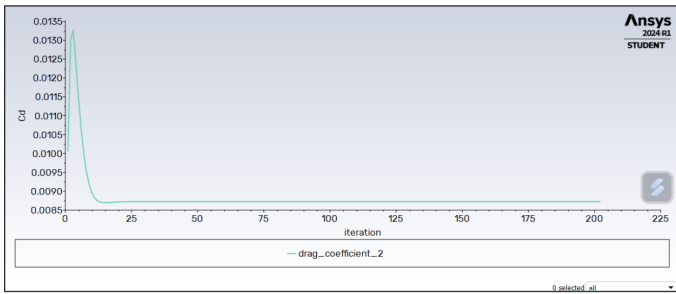


Figure 5. 3.4 Cl plot for nodes = 17280

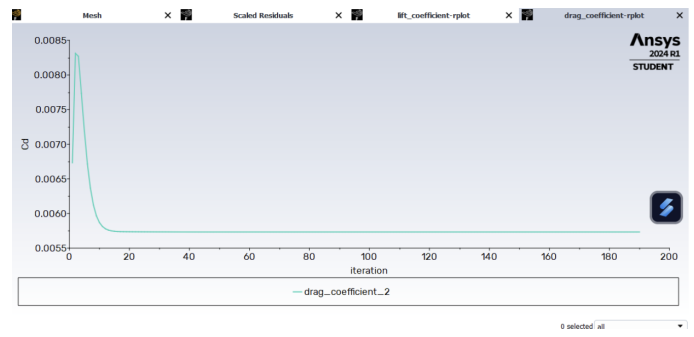


Figure 10. 3.9 Cd plot for nodes = 68160

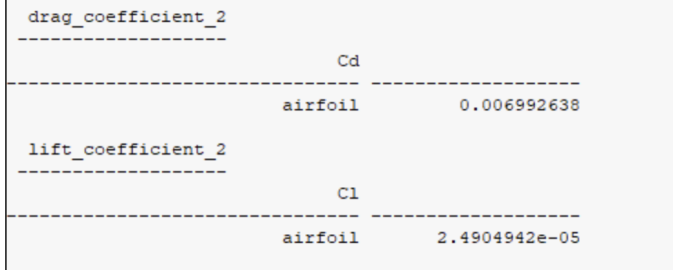


Figure 6. 3.5 Cd and Cl value for normal

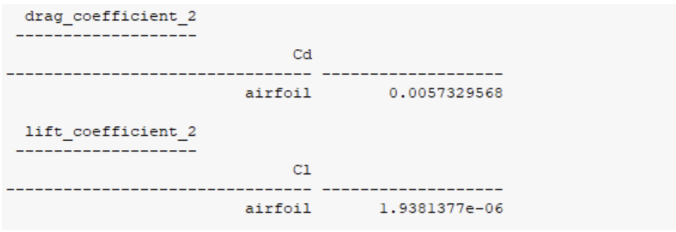


Figure 7. 3.6 Cd and Cl value for normal for node = 68160

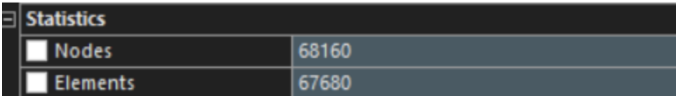


Figure 8. 3.7 Elements and Nodes

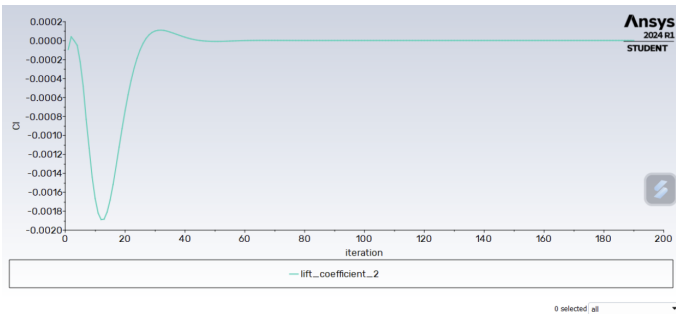


Figure 9. 3.8 Cl plot for nodes = 68160

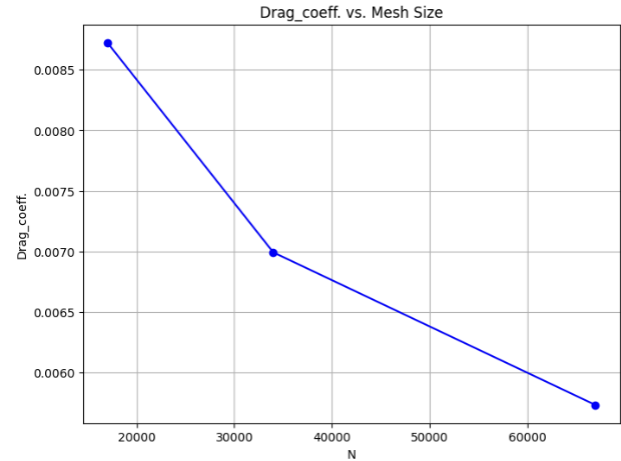


Figure 11. 3.10 Drag Coefficient Vs Mesh Size

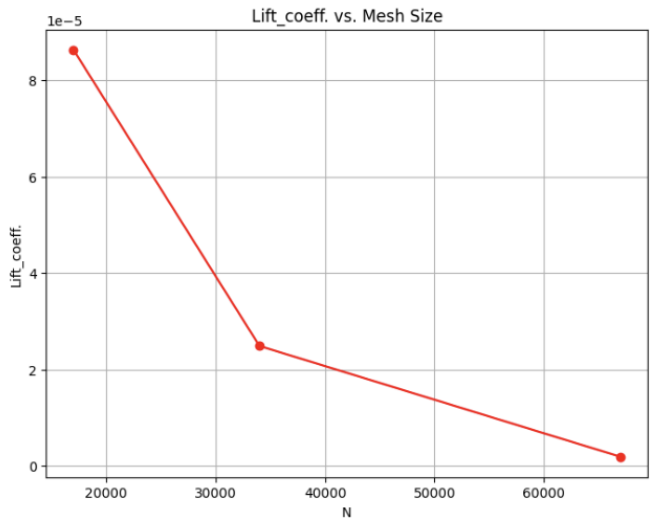


Figure 12. 3.11 Lift Coefficient Vs Mesh Size

4. Discretisation Schemes and Solution Methodology

4.1. Discretisation Schemes

In the computational fluid dynamics (CFD) simulation, the discretisation schemes play a critical role in approximating the continuous governing equations of fluid flow on a discrete grid. The discretisation schemes determine how the spatial and temporal derivatives in the governing equations are approximated

and computed numerically. In this study, the following discretisation schemes are employed:

- Spatial Discretisation:

- Finite Volume Method (FVM): The governing equations, namely the Navier-Stokes equations, are discretised using the finite volume method. In FVM, the computational domain is divided into control volumes, and the integral form of the governing

equations is applied to each control volume. This approach conserves mass, momentum, and energy within each control volume, making it well-suited for fluid flow simulations.

- Temporal Discretisation:

- Steady-State Simulation: The simulation is conducted in a steady-state regime, where the flow variables remain constant with time. Therefore, no temporal discretisation is required for time-dependent terms in the governing equations.

4.2. Solution Methodology

The solution methodology refers to the numerical techniques and algorithms used to solve the discretised equations and obtain the numerical solution for the flow field. The following solution methodology is employed:

Solver: Ansys Software: The simulation is performed using the Ansys software suite, which provides powerful tools for conducting CFD simulations. Ansys offers a range of solvers and numerical methods tailored for various fluid flow problems. In this study, Ansys is utilized to solve the discretised continuity, x-momentum and y-momentum equations (Navier-Stokes Equations) and obtain numerical solutions for the flow field.

The Scheme used here is COUPLED.

For laminar flow simulations, we used the Finite Volume Method (FVM) to discretize the Navier-Stokes equations.

We chose the Pressure-Based solver in Ansys Fluent to solve the incompressible Navier-Stokes equations.

5. Results and Discussion

5.1. Create a 2D computational domain including the NACA 0012 airfoil section at 0° angle of attack. Apply appropriate boundary conditions (inlet, outlet, and symmetry or wall boundaries).

For 0° angle of attack,

Inlet Boundary Condition: x-Velocity 30 m/s, y-velocity= 0°

Wall Boundary Condition: No slip condition for airfoil.

5.2. Calculate drag coefficient (C_D) and lift coefficient (C_L) for 0° angle of attack (AOA).

From the graphs, we find that the coefficient of drag, $C_D = 0.007$ and coefficient of lift, $C_L = 0$. This can also be verified from ANSYS compute.

5.3. Perform mesh independence study

A mesh independence study is conducted to ensure the reliability and accuracy of the simulation results.

Results obtained from different levels of mesh refinement are compared to assess mesh independence.

It is observed that the mesh attains independence on refinement.

5.4. Simulate for 5° AOA and calculate drag and lift coefficients

For 5° angle of attack,

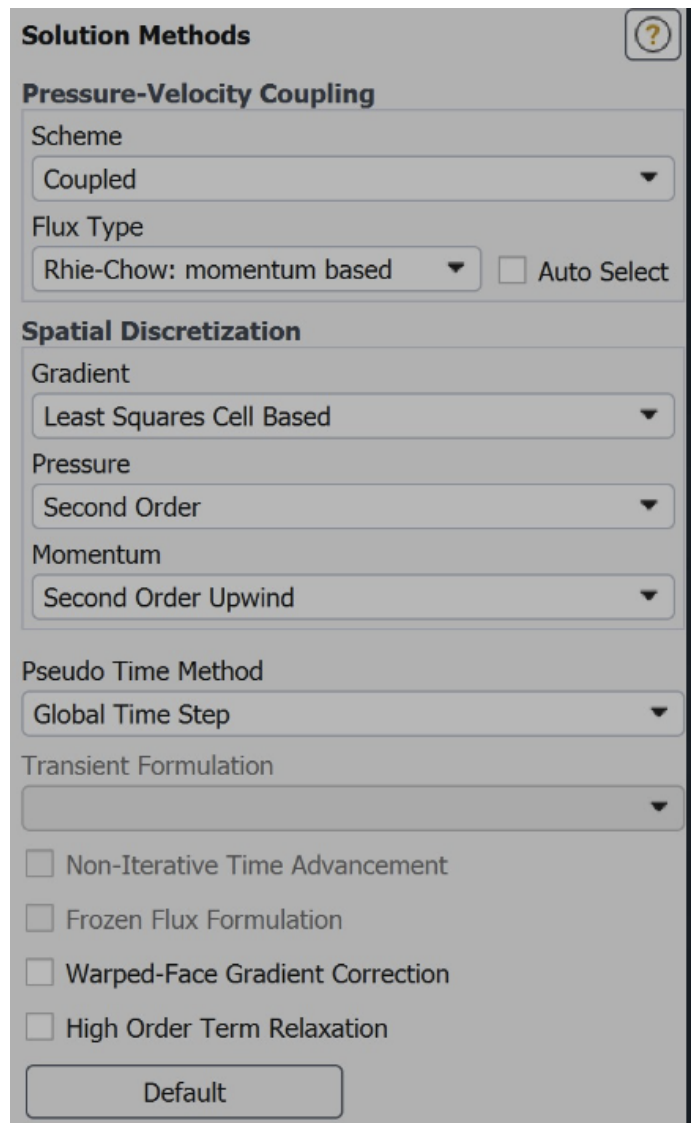


Figure 13. 4.1 ANSYS Solution Method

Inlet Boundary Condition: x-Velocity 29.885 m/s, y-velocity= 2.615 Wall Boundary Condition: No slip condition for airfoil.

We do not see convergence for 5° AOA. The reason could be that it could be encountering transient flow phenomena. These transient effects can cause the oscillation behaviour for iteration as the solver attempts to resolve the dynamic flow behavior accurately.

5.5. Tabulate your results for 0° and 5° AOA and compare your results with the literature.

Comparing the ANSYS results and the literature, we find that the results are same for 0° AOA. While, for 5° AOA, the results fall within the expected range.

AOA	Parameters	Ansys – CFD results	Literature
0°	CD	0.007	0.0065
0°	CL	0	0
5°	CD	0.02 - 0.14	0.006
5°	CL	-0.2 - 0.5	0.5

Table 2. C_D and C_L for different AOA

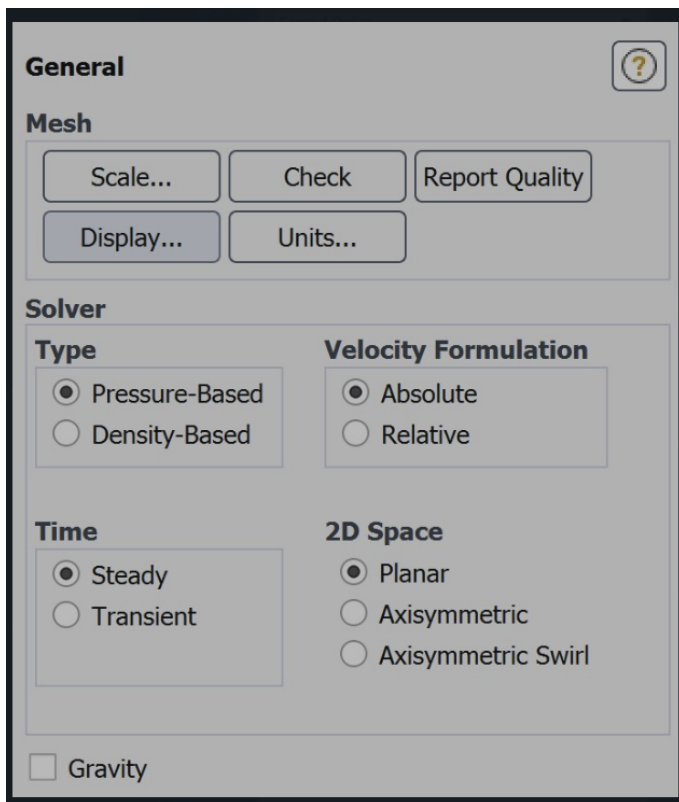


Figure 14. 4.2 ANSYS Solver

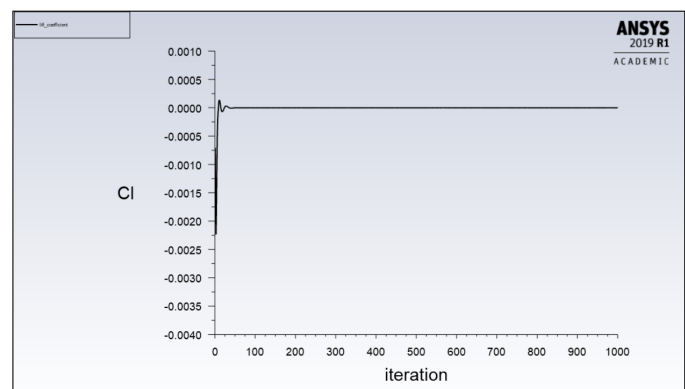


Figure 17. 5.2.2 Coefficient of Lift

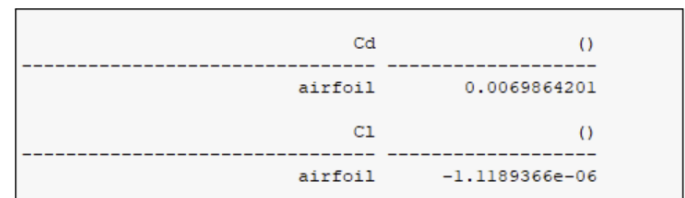


Figure 18. 5.2.3 Results from ANSYS compute

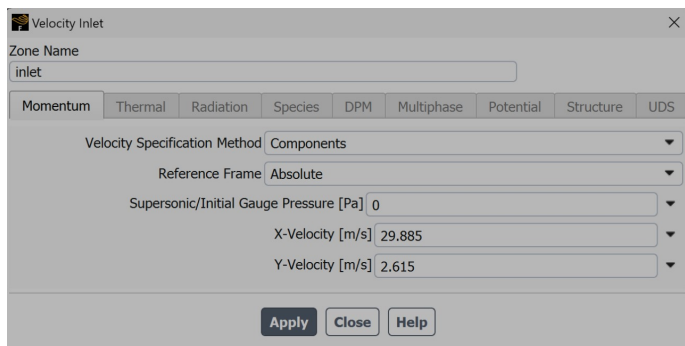


Figure 19. inlet velocity for 5° AOA

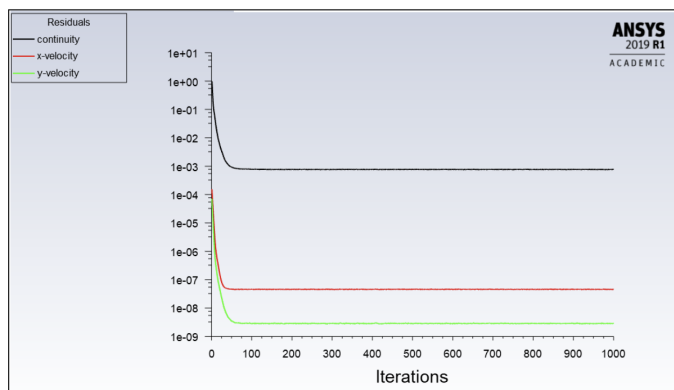


Figure 15. 5.1.1 Continuity, x-velocity, and y-velocity calculations for 0° AOA

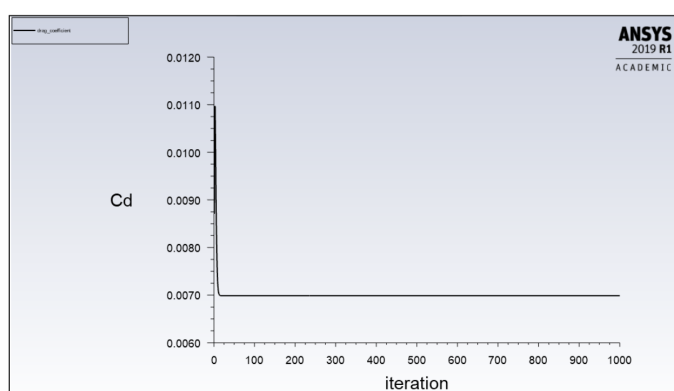


Figure 16. 5.2.1 Coefficient of Drag

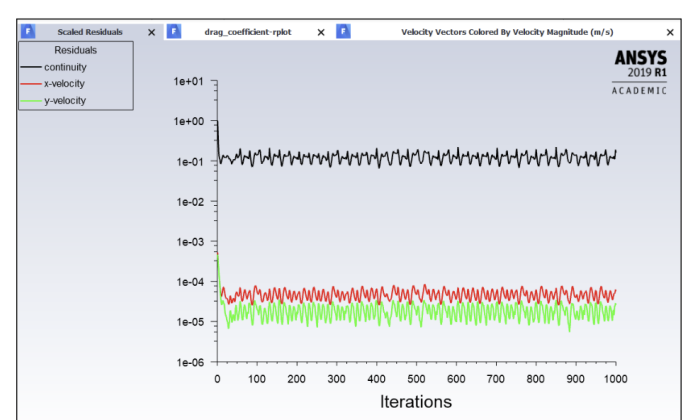


Figure 20. 5.4.1 Continuity, x-velocity, y-velocity for 5° AOA

5.6. Plot the velocity, pressure and streamline contours separately.

The analysis of velocity contours revealed distinct patterns of airflow around the airfoil. Higher velocities were consistently observed over the upper surface of the airfoil, indicative of accelerated airflow. Conversely, lower velocities were evident

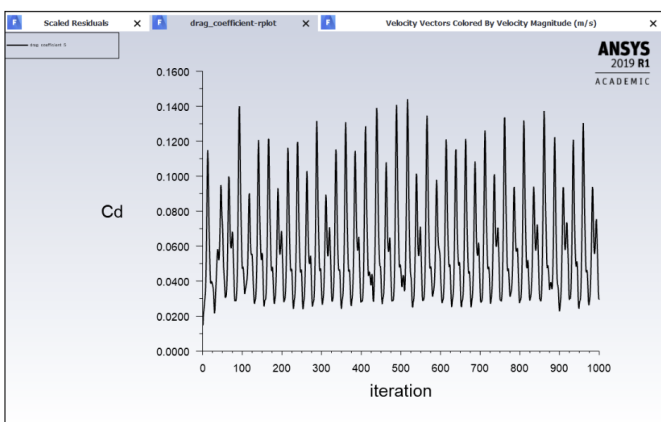


Figure 21. 5.4.2 Cd for 5° AOA

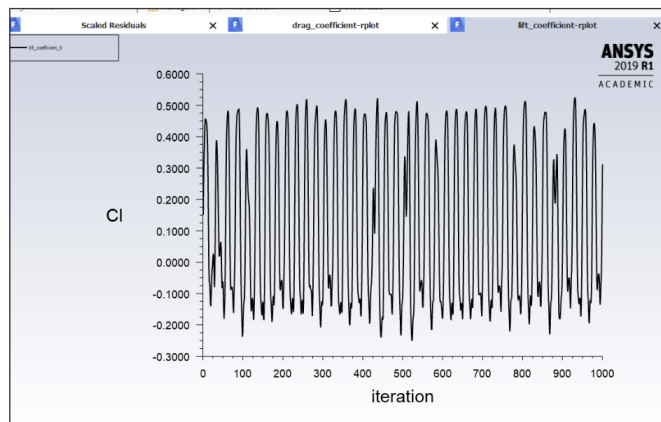


Figure 22. 5.4.3 Cl for 5° AOA

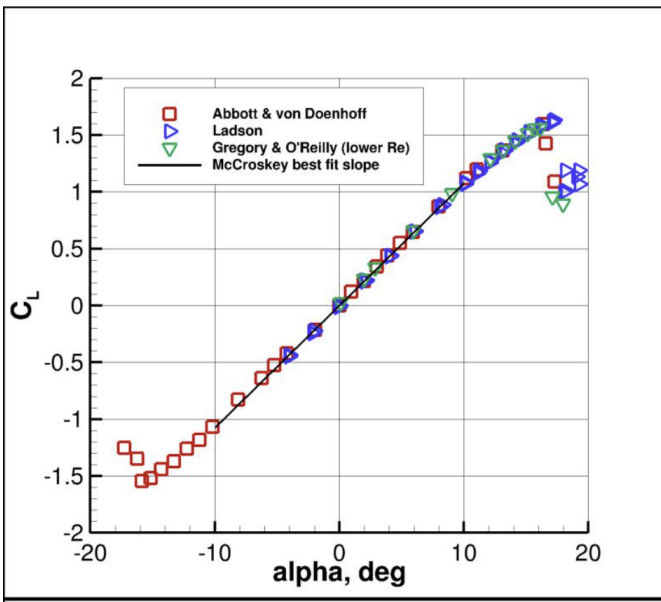


Figure 23. 5.5.1 Cl vs alpha (AOA)

beneath the airfoil, reflecting deceleration due to the airfoil's shape. These variations in velocity distribution play a crucial role in generating lift and influencing the overall aerodynamic performance of the airfoil.

The pressure contours revealed notable pressure gradients across the airfoil's surface. Lower pressures over the upper

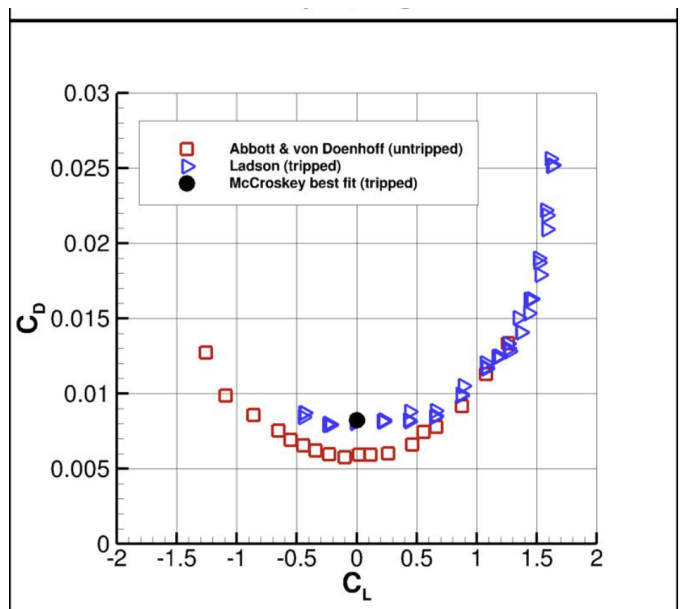


Figure 24. 5.5.2 Cd vs Cl

surface indicated areas of lift generation from accelerated air flow, while higher pressures underneath contributed to drag. These insights into pressure distribution offer valuable understanding of aerodynamic forces and flow patterns around the airfoil.

Streamline contours provided a detailed view of flow dynamics around the airfoil, showing the paths of fluid particles. They depicted boundary layer formation, flow separation, and vortex development. Variations in curvature and separation patterns, especially with different angles of attack, indicated changes in aerodynamic performance and flow behaviour.

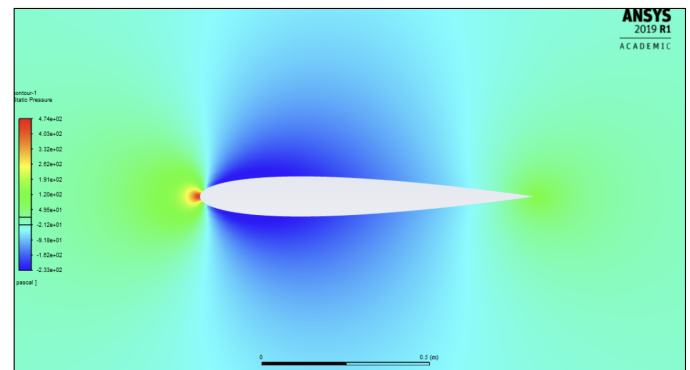


Figure 25. 5.6.1 Pressure Contour for 0° AOA

5.7. Mark and describe the flow features in the contours (including boundary layer and flow separation if any).

- Boundary Layer Formation: Air adheres to the airfoil's surface, forming a thin layer called the boundary layer, which may transition from laminar to turbulent along the airfoil's length.
- Flow Acceleration: The airfoil's shape accelerates airflow over its curved upper surface while decelerating it on the lower surface, generating lift due to pressure differences.
- Stagnation Point and Separation: At the leading edge, the airflow splits, with some passing over the upper surface

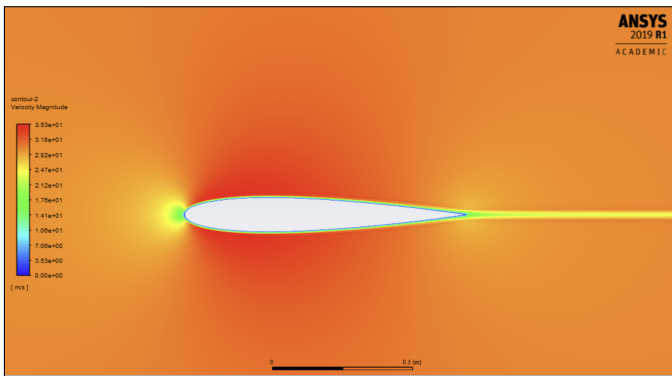


Figure 26. 5.6.2 Velocity Contour for 0° AOA

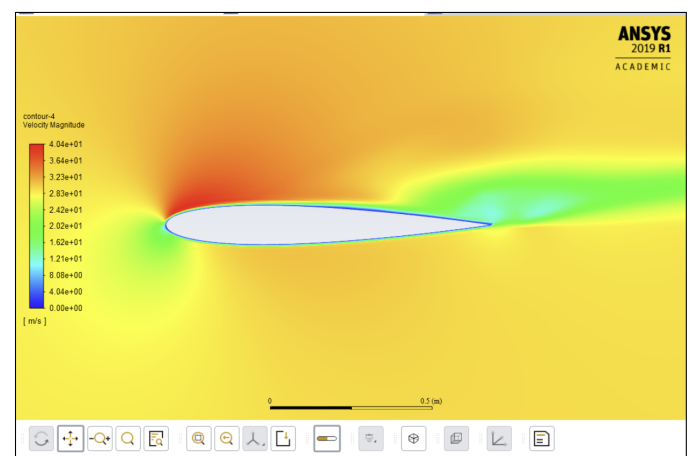


Figure 29. 5.6.5 Velocity Contour for 5° AOA

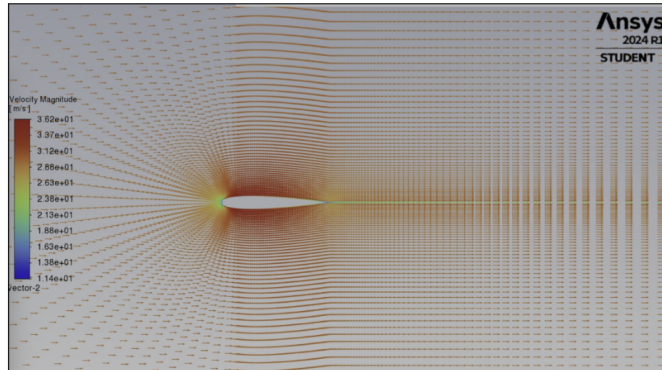


Figure 27. 5.6.3 Streamline Contour for 0°

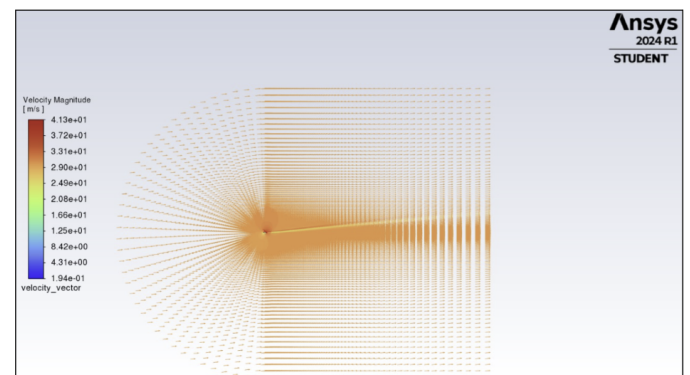


Figure 30. 5.6.6 Streamline Contour for 5° AOA

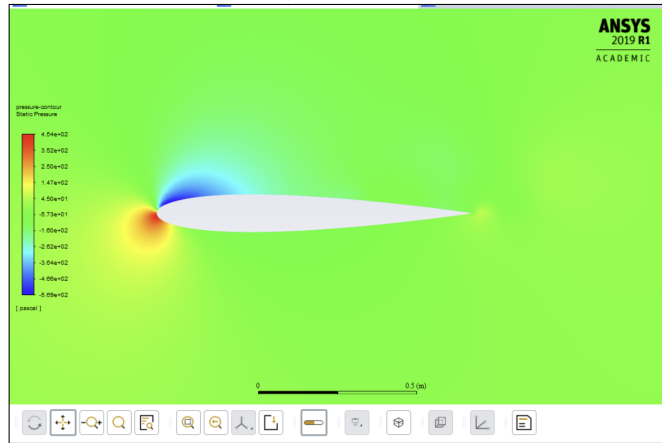


Figure 28. 5.6.4 Pressure Contour for 5° AOA

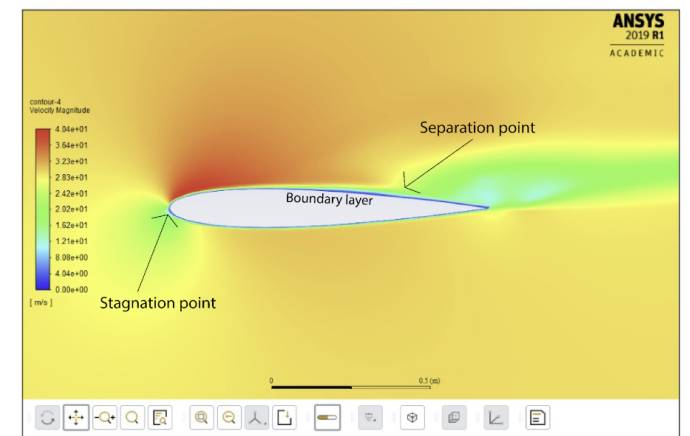


Figure 31. 5.7.1 Flow features

and some beneath the lower surface. Increased angle of attack can lead to flow separation, where airflow detaches from the surface, causing loss of lift and increased drag.

- Boundary Layer Separation: Flow separation typically starts at the trailing edge due to abrupt pressure changes, creating a region of recirculating flow known as the wake, which increases drag.

6. Conclusion

The simulation provides valuable insights into the aerodynamic behavior of the NACA 0012 airfoil under laminar flow conditions. The drag and lift coefficients, along with the visualization of flow features, offer a comprehensive understanding

of the airfoil's performance.

The mesh independence study demonstrated the convergence of results, enhancing confidence in the obtained outcomes.

The results revealed significant findings regarding the aerodynamic characteristics of the NACA 0012 airfoil, particularly at 0° and 5° angles of attack. The calculated drag and lift coefficients were compared with literature values, indicating good agreement and validating the simulation approach. Furthermore, the velocity, pressure, and streamline contours provided detailed visualizations of the flow field, enabling the identifica-

tion of key flow features such as boundary layer development and potential separation points.

7. References

- Turbulence Modeling Resource: https://turbmodels.larc.nasa.gov/naca0012_val.html